Controllable conversion of cellulose nanocrystals to cellulose microspheres: Insight on the effect of parameters during spray drying

QINGJUN MENG, WENLIANG ZHENG, AND YANG XU

ABSTRACT: Cellulose microspheres, which have mainly been produced via the sol-gel method up until now, exhibit a promising potential for broad applications due to their regular microstructure and renewability. However, some issues with production of cellulose microspheres, such as the recycling of involved organic solvents and the removal of the residual solvents, should be solved.

In this study, a cellulose nanocrystals (CNCs) suspension was used to produce cellulose microspheres via spray drying in order to avoid the use of organic solvents. The effects of CNCs particle size, CNCs concentration, and inlet temperature of spray drying on microstructure and particle size of cellulose microspheres were investigated. The results indicated that the optimal average particle size and concentration of CNCs used for obtaining cellulose microspheres were 106 nm and 0.1 wt%, respectively. Under the optimal conditions, cellulose microspheres with a regular spherical morphology and an average particle size of ca. 3 μm were obtained. The sulfuric acid hydrolysis and spray drying process barely affected the crystalline structure of cellulose. However, the introduced sulfhydryl groups, which were confirmed by Fourier transform infrared spectroscopy results, degraded the thermostability of cellulose. Generally speaking, converting CNCs to cellulose microspheres via spray drying is beneficial for promoting the controllable and continuous production of cellulose microspheres.

Application: This paper focuses on the controlled preparation of cellulose microspheres. The morphology and structure of cellulose microspheres were regulated by controlling the size of CNCs, the concentration of CNCs, and the inlet temperature of spray drying, providing a wider application potential for cellulose.

In recent years, microspherical structured materials have garnered widespread attention due to their unique structural characteristics, tunable pore size distribution, and high specific surface area [1,2]. The raw materials for preparing microspheres are diverse, including natural polymers [3,4], synthetic polymers[5], and inorganic materials [1]. Natural polymer materials, such as cellulose, starch, and chitosan, exhibit significant advantages in microsphere preparation due to their abundant resources, excellent biocompatibility, and biodegradability. In particular, the utilization of cellulose for the purpose of replacing non-renewable resources is crucial in addressing global environmental degradation and resource scarcity due to its widespread availability and accessibility.

Various forms and structures of cellulose-based materials have been developed, including aerogels, hydrogels, and microspheres [6,7]. Among them, cellulose microspheres, as a unique form, demonstrate broad application prospects in adsorption or as carriers, as well as pharmaceutical transportation, due to their high specific surface area, small size, and ease of transport [8]. Furthermore, the surface of cellulose microspheres is rich in -OH groups, which can be modified chemically or physically to obtain new functional properties [8]. Zhu et al. [9] prepared hydrangea-like cellulose microspheres using an emulsion method. The microspheres exhibited a stable three-dimensional network porous structure, demonstrating adsorption capacities of 412.1 mg/g and 286.5 mg/g for methylene blue (MB) and methyl orange (MO) under neutral conditions. Pei et al. [10] utilized porous cellulose microspheres as carriers to prepare highly dispersed palladium (Pd) nanocatalysts. The nanoporous structure of the cellulose microspheres facilitates the adhesion and dispersion of Pd particles, while their abundant hydroxyl groups can effectively fix the Pd particles. Wu et al. [11] employed sol-gel method combined with esterification reaction to prepare phosphorylated cellulose microspheres used for the loading and release of ciprofloxacin.

Up until now, cellulose microspheres have mainly been produced via the sol-gel method, which usually involves the use of organic solvents and surfactants. Organic solvents and surfactants used in abundance are going against the development of green chemistry. Furthermore, organic solvents and surfactants are difficult to eliminate completely. The residual organic solvents or surfactants may be a disadvantage for the further application of cellulose microspheres. Therefore, it is of great significance to find a sat-

isfactory method that complies with development of green chemistry to obtain cellulose microspheres.

Spray drying is a green and efficient drying technology that has been extensively used in the food and medicine industries and can quickly dry liquids with high water content for easy transportation and storage [12]. The particles in suspension/solution (to be dried) are expelled through a nozzle and come into contact with hot gas [13,14]. The medium of suspension, like water, vaporizes at this point, enabling the production of dried particles [15,16]. For the production of cellulose microspheres, the approach that uses spray drying to obtain cellulose microspheres from nanocellulose is very promising.

Previous researchers spent great effort on the spray drying of nanocellulose, including the enhancement of redispersibility [17] and the variation in microstructure/particle size/surface energy of nanocellulose [18-21]. Peng et al. [18,20-22] have done a lot of work in this respect, and they found that the variation of spray drying parameters was crucial for the microstructure of spray-dried nanocellulose. The microstructure of spray-dried CNCs include mushroom cap-like, doughnut-like, spherical, cellulose bundle-like, and irregular agglomerated particles, etc. [21,22]. Cellulose nanofibrils (CNFs) are more inclined to form cellulose fiber bundles and irregular agglomerated particles, while CNCs with smaller size tend to form mushroom cap-shaped, doughnut-shaped, and spherical particles [18]. Among them, spherical CNCs flocculants obtained via spray drying are more attractive for downstream utilization, which may have a positive application prospect in, for instance, drug carriers and adsorptions [23,24]. Unfortunately, systematic research involving the controllable conversion of CNCs to cellulose microspheres is absent. It should be noted that many factors will affect the final morphology of spray-dried samples, such as drying temperature, suspension concentration, and properties of the raw materials.

In this study, spray drying was used for the controllable conversion of CNCs to cellulose microspheres. The primary aim of this research is to find the critical conditions for the controllable conversion of CNCs to cellulose microspheres. Hence, the effect of essential indicators, such as the particle size of CNCs, the drying concentration of CNCs, and the spray drying temperature, on the microstructure, particle size distribution, chemical/crystalline structure, and thermostability of dried CNCs were investigated.

MATERIALS AND METHODS

Materials

The bleached kraft softwood pulp was purchased from Qingshan Paper Industry Co. Ltd. (Fujian, China). Sulfuric acid (98 wt%, AR) was purchased from Dongda Chemical Co. Ltd. (Kaifeng, China). Deionized water was used to disperse CNCs, and all deionized water was prepared using a Milli-Q system (MilliporeSigma; Burlington, MA, USA) with a resistivity of 15 MΩ·cm.

Preparation of CNCs suspension

The bleached kraft softwood pulp was split manually and then crushed by a micro plant crusher FZ102 (Beijing Zhongwei Instrument Co. Ltd; Beijing, China) to achieve a fiber size of ca. 1.5 mm. The crushed cellulose powder was mixed with 64 wt% sulfuric acid with a liquid-solid ratio of 10:1 in a flask. The mix was stirred for 2~3 min to ensure the homodispersing of cellulose powder. Then, the flask was put into a water bath with a temperature of 45°C to hydrolyze cellulose for a predetermined time (30, 50, 70, or 90 min). Upon completion, deionized water was used to dilute the reacting mixture and terminate the hydrolysis reaction, obtaining a uniform suspension (containing CNCs). The suspension was centrifuged at 10000 rpm for 15 min by an LD-2A centrifuge (Beijing Zhongyi Zhonghe Biotechnology Co. Ltd.; Beijing, China). The separated precipitates (including CNCs) were centrifuged and washed continuously until the pH value of the supernatant was 5.0~6.0. The final precipitates obtained were dialyzed against deionized water by a Biosharp cellulosic dialysis bag (Labgic Co. Ltd.; Beijing, China) with molecular weight cutoff of 14000 until the conductivity of suspensions had approached that of deionized water. In the end, the CNCs suspension was stored at 4°C for further treatments and tests. The suspension should be mildly sonicated to disperse CNCs and diluted to the required concentration before spray drying. **Figure 1** provides a schematic of the process to fabricate cellulose microspheres.

Conversion of CNCs to cellulose microspheres via spray drying

The effect of CNCs particle size, CNCs concentration, and inlet temperature of spray drying on the morphology and structure of CNCs aggregations was investigated. The CNCs suspension was spray-dried by a SD-Basic spray dryer (LabPlant; Hunmanby, UK), which is equipped with a nozzle (0.5-mm diameter) with a flow rate of hot gas of 9 L/min and a rate of feed of 7 mL/min.

To investigate the conversion effects of CNCs with different particle sizes, CNCs subjected to varied sulfuric acid hydrolysis times were utilized, with a CNCs concentration of 0.1 wt and an inlet temperature of 180°C. To explore the effect of CNC concentration on the morphology and structure of cellulose microspheres, the CNC mass concentrations were varied at 0.05 wt%, 0.1 wt%, 0.3 wt%, 0.5 wt%, 1 wt%, and 1.5 wt%, with a sulfuric acid hydrolysis time of 70 min and an inlet temperature of 180°C. Further investigation into the effect of inlet temperature/CNCs concentration on the morphology and structure of cellulose microspheres was carried out with varied CNCs concentrations (0.02 wt%, 0.05 wt%, and 0.08 wt%) and inlet temperatures (140°C, 160°C, and 180°C), with a sulfuric acid hydrolysis time of 70 min.

Characterizations

The microstructure of CNCs was observed by a Thermo Fisher Scientific (Waltham, MA, USA) Tecnai G2 F20 S-

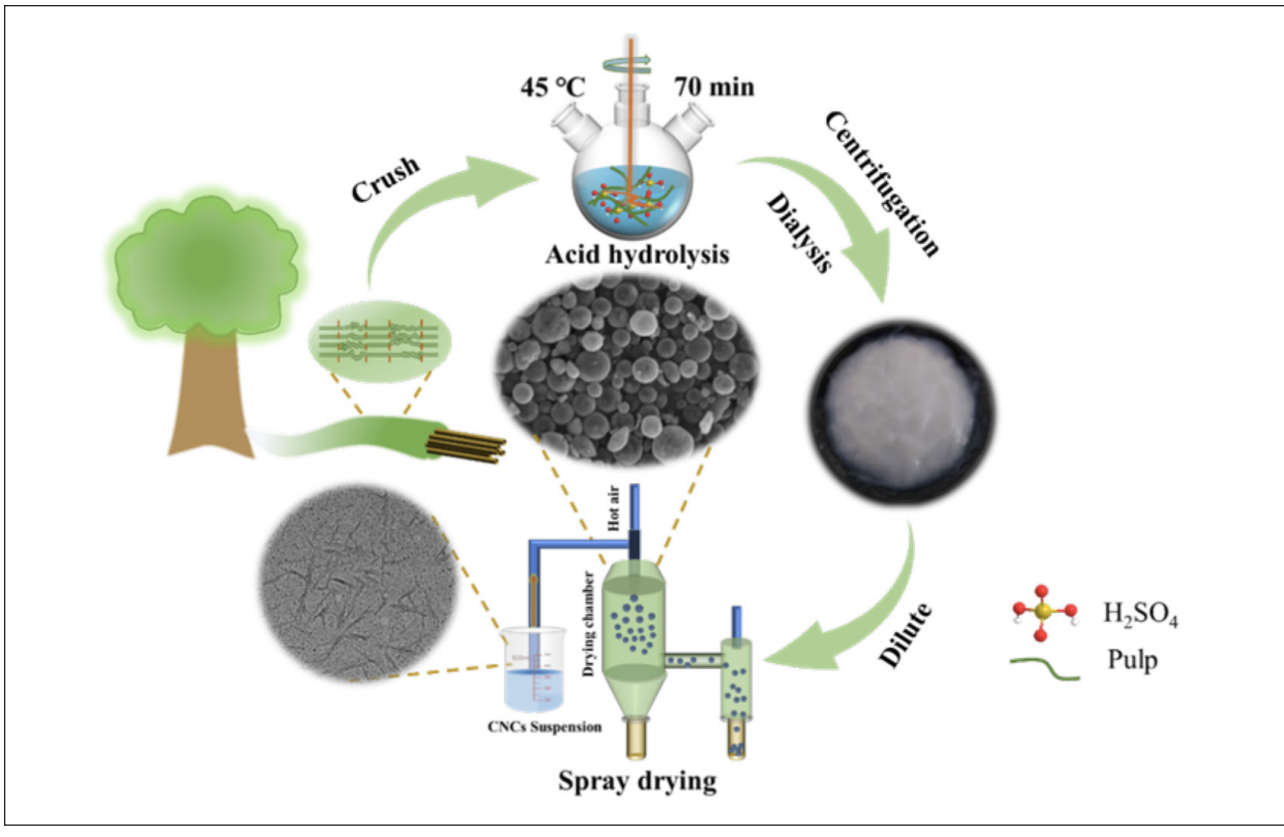

1. Schematic illustrating the process to fabricate cellulose microspheres (H_2SO_4: sulfuric acid).

TWIN transmission electron microscope (TEM). The preparation procedure of specimens used for TEM observation was as follows: 20 µL of CNCs suspension, which was diluted to 0.01 wt% by deionized water, was transferred onto a carbon-supported copper grid, and then the grid was dried naturally in a fume hood before TEM observation.

The particle size and size distribution of CNCs were detected by Zetasizer Nano ZS (Malvern Panalytical; Malvern, UK). The CNCs suspension, with a concentration of 0.15 wt% diluted by deionized water, was ultrasonically treated (150 W, 20 kHz) for 10 min before analysis.

The morphology of cellulose microspheres was observed using a TESCAN (Brno, Czechia) VEGA 3 SBH scanning electron microscope (SEM) with an acceleration voltage of 15 kV. The dried samples were coated onto conductive adhesive containing copper pieces, which were then attached to the sample stage. Prior to observation, the surfaces of specimens were coated with platinum under vacuum for 60 s.

The particle size and size distribution of spray-dried CNCs aggregations were detected by a Bettersizer 3000 Plus particle sizer (Bettersize Instruments; Dandong, China). The spray-dried CNCs to be tested were uniformly mixed in deionized water, and then this suspension was added to the sample pool to ensure the obscuration was between 10%~30%. Subsequently, an ultrasonic generator was activated to ensure complete dispersion of the sample, followed by the initiation of the measurement.

The chemical structure of cellulose fibers and CNCs and their aggregations was determined by Fourier transform infrared spectroscopy (FTIR) using a Vertex 70v spectrometer (Bruker Scientific Instruments; Billerica, MA, USA) with a range of 4000 to 400 cm^{-1} for 32 scans using the KBr pellet method.

The thermostability of cellulosic specimens was determined by an STA 449F thermal analyzer (Netzsch; Selb, Germany) in nitrogen at a temperature range from 40°C to 800°C with a heating rate of 10°C/min and a nitrogen flow rate of 50 mL/min.

The crystal structure of cellulosic specimens was characterized using a Bruker D8 Advance X-ray diffractometer (XRD) equipped with Cu Kα radiation (k = 1.54 A˚) as the X-ray resource and operating at 40kV and 30mA with a scan rate of 0.05/s in a 2θ range at 5° to 90°. The crystal index of specimens was calculated according to the method reported by Segal et al. [25] using Eq.1:

$$\text{Cellulose I:} CrI = \frac{I_{200} - Iam}{I_{200}} \times 100\% \quad (1)$$

where I_{200} is the maximal diffraction intensity of the XRD pattern, which is usually present at a 2θ range of 22.3–22.8, and I_{am} is the diffraction intensity at 2θ = 18.0.

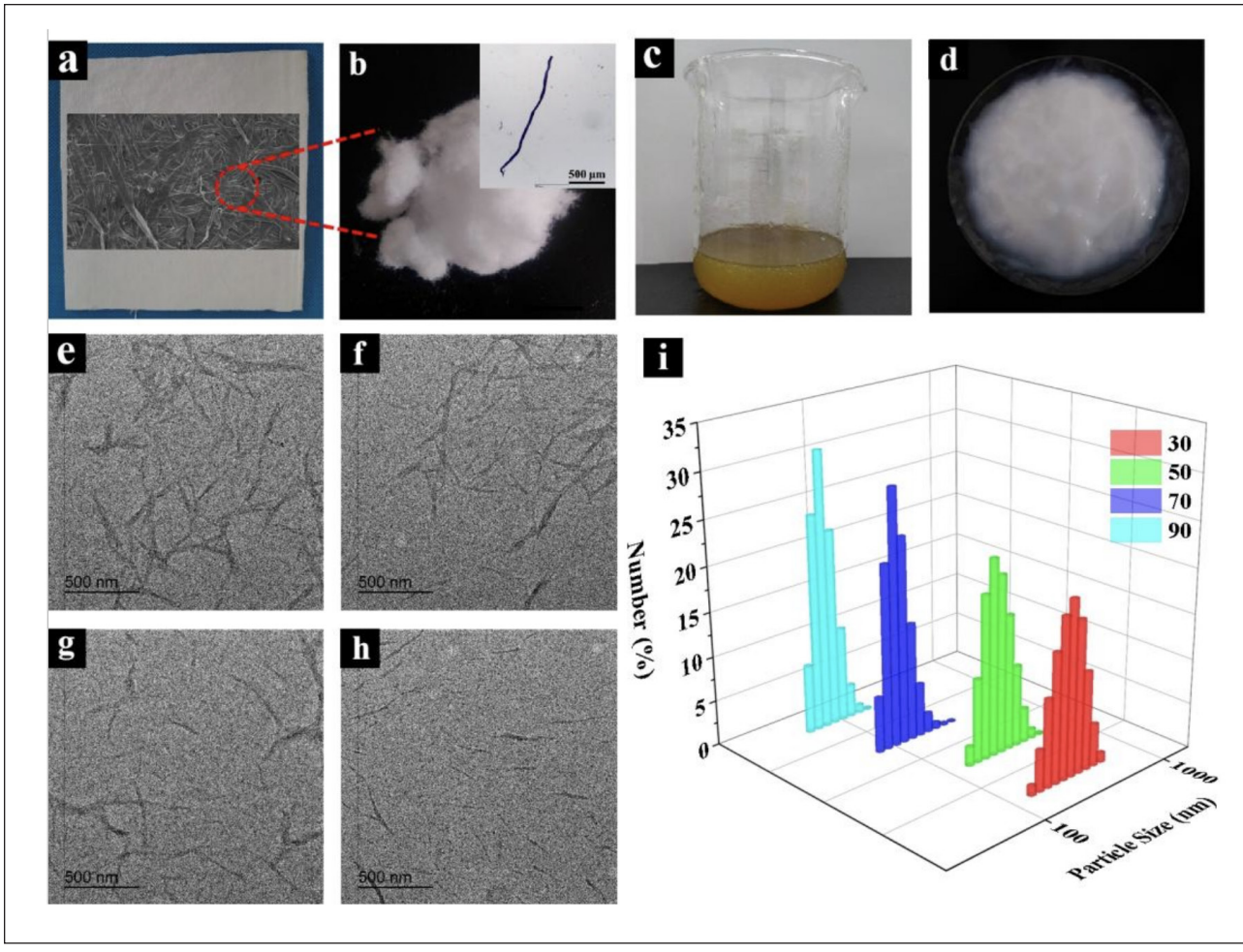

2. Size and morphology of cellulose nanocrystals (CNCs): (a)–(d) macromorphology of softwood fibers and CNCs; (e)–(h) transmission electron microscope (TEM) images of CNCs at 30 min, 50 min, 70 min, and 90 min; and (i) particle size distribution of CNCs.

RESULTS AND DISCUSSION

Effect of spray drying parameters on microstructure of cellulose microspheres

During spray drying, the surface water of minute hydrous particles dries first, and then interior water diffuses toward the surface. Both capillary forces and diffusion forces, which are respectively determined by the evaporation rate and diffusion rate, define the resultant shape of spray-dried CNC particles [26]. These forces can be regulated by both the inlet temperature of spray drying and the concentration of the CNCs suspension. Additionally, the average particle size of CNCs is also a crucial factor. As the hydrous droplets gradually shrink during the rapid spray drying process, the presence of larger CNCs may lead to the formation of bulges on the surface, making it difficult to obtain cellulose microspheres with uniform morphology. Due to the significant impact of the inlet temperature of spray drying, CNCs concentration, and average particle size on the morphology of cellulose microspheres formed from CNCs, this study mainly investigates the effects of these three parameters.

The CNCs with varied average particle size were obtained by controlling the reaction time of sulfuric acid hydrolysis on cellulose. The variation of CNCs preparation, including macro-morphology, microstructure, average particle size, and size distribution of CNCs, is shown in **Fig. 2**. In general, the obtained CNCs exhibit a homogeneous size distribution. With the acid hydrolysis time increasing from 30 min to 90 min, the average particle size of CNCs decreased from 295 ± 0.09 nm to 79 ± 0.05 nm (Fig. 2).

The obtained CNCs suspension was spray-dried (180°C, 0.1 wt%), and the microstructure of the obtained cellulose microspheres is shown in **Fig. 3**. The CNCs with the largest average particle size of 295 ± 0.09 nm when hydrolysis time was shortest (30 min) were adopted. The spray-dried CNCs, for this case, exhibit multifarious microstructure (Fig. 3a). Unfortunately, cellulose microspheres, i.e., CNCs aggregations with regular sphericity, were scarcely observed (Fig. 3a). With the decrease of CNCs particle size, the microstructure of spray-dried CNCs aggregations became more and more regular. It is worth noting that relatively regular cellulose microspheres were obtained (Fig. 3c and

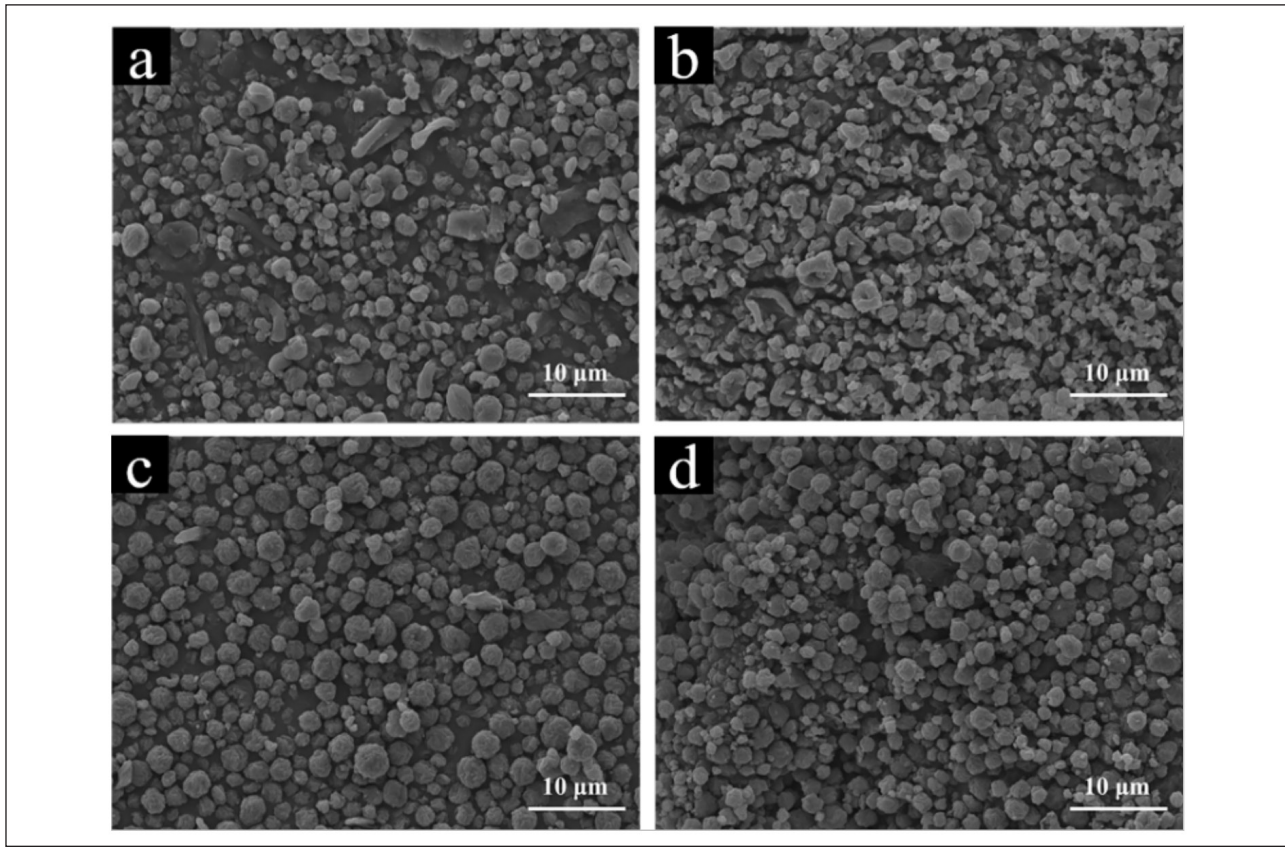

3. Scanning electron microscope (SEM) images of cellulose microspheres at varying sulfuric acid hydrolysis times: (a) 30 min, (b) 50 min, (c) 70 min, and (d) 90 min.

Fig. 3d) when the average particle size of CNCs was lower than 110 nm (with a hydrolysis time higher than 70 min). The spray drying process of CNCs suspension can be considered as the rapid drying of dispersed droplets consisting of CNCs suspension. The microstructure of spray-dried CNCs is decided by the individual dried droplets. The separated droplets were shrunken continually during the spray drying process. The CNCs with large particle sizes cannot be arranged within the droplet consistently. The droplet containing CNCs with large particle sizes will be punctured at an unspecified time point during spray drying. As a result, the microstructure of spray-dried exhibited irregular morphology, and cellulose microspheres cannot be obtained. Therefore, the decreased CNCs average particle size is beneficial for the formation of cellulose microspheres from CNCs via spray drying. Unfortunately, the yield of CNCs usually decreases with the prolonged time of sulfuric acid hydrolysis. Hence, the time of sulfuric acid hydrolysis should be shortened as much as possible on the basis that cellulose microspheres can be formed. In the following research, 70 min sulfuric acid hydrolysis time was adopted.

The concentration of CNCs suspension also affects the conversion of CNCs into cellulose microspheres. The effect of CNCs concentration on the microstructure of cellulose microspheres was shown in **Fig. 4**. Regular cellulose microspheres with uniform morphology and structure were obtained when a lower CNCs concentration was adopted (0.05 wt% and 0.1 wt% in Fig. 4a and Fig. 4b, respectively). Unfortunately, surface indentations can be observed in the SEM image of dried CNCs with an initial concentration of 0.05 wt% (Fig. 4a). With the increase of CNCs concentration (0.3 wt% and 0.5 wt% in Fig. 4c and Fig. 4d, respectively), the cellulose microspheres evolve from a regular spherical form to irregular morphology, i.e., the inhomogeneous particle sizes and shapes. Nevertheless, near-spherical particles can be observed in the SEM images. With the further increase of CNCs concentration (1.0 wt% and 1.5 wt% in Fig. 4e and Fig. 4f, respectively), spherical particles can be scarcely observed in the SEM images, and sheet-like CNCs aggregations were detected.

During spray drying, CNCs suspension is passed through a circular nozzle to form a suspended film. The high-speed hot air continues to break the suspended membrane into ligaments, which then form droplets with diameters ranging from a few micrometers to tens of micrometers. Due to the increased hydrophilicity of the CNCs, the formation process of droplets is affected when a high concentration of CNCs suspension (higher than 1 wt%) is adopted [18,26,27]. The suspended membrane cannot be broken down thoroughly, finally leading to the formation of sheet-like CNCs aggregations (Fig. 4e and f). As mentioned, the surface water of droplets was evaporated first during

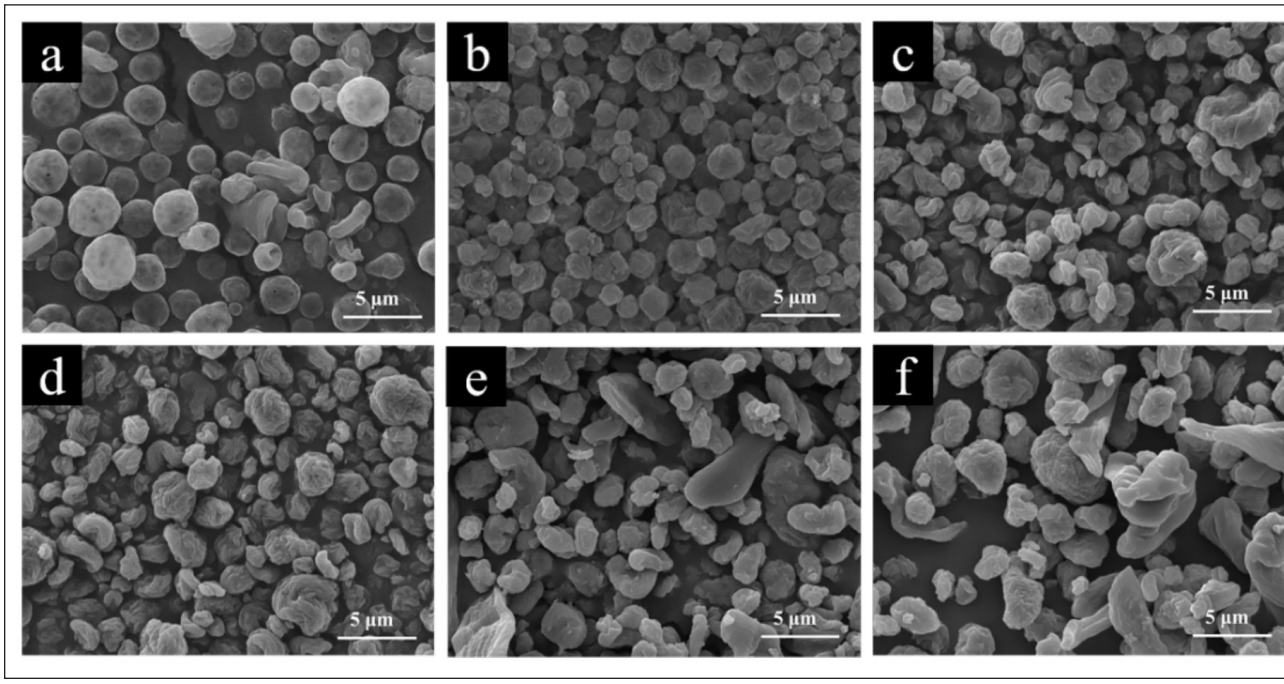

4. The SEM images of cellulose microspheres prepared with varying concentrations of CNCs: (a) 0.05 wt%, (b) 0.1 wt%, (c) 0.3 wt%, (d) 0.5 wt%, (e) 1 wt%, and (e) 1.5 wt%.

spray drying. The further evaporation of the inner water will be affected by the dried surface. When a low concentration of CNCs was adopted, the dried surface was too thin to be preserved. The spherical surface structure is destroyed by the continual evaporation of inner water, resulting in a surface-sunken spherical particle (Fig. 4a). When a comparatively high concentration of CNCs was adopted (0.3 wt% and 0.5 wt%), the thickly dried surface cannot be destroyed by the evaporation of inner water. Unfortunately, the evaporation rate of inner water will be affected, resulting in a prolonged drying process, which may cause the rewet of surface and eventual formation of the irregular particles.

There is evidence that, as discussed previously, the dilute CNCs suspension with a concentration lower than 0.1 wt% is favorable for the formation of cellulose microspheres by spray drying. Hence, further investigation was carried out to reveal the effect of inlet temperature on the microstructure of cellulose microspheres under a low concentration of CNCs (0.02 wt%, 0.05 wt%, and 0.08 wt%), as shown in **Fig. 5**. In general, following spray drying, spherical and irregular CNCs aggregations can form from rod-like CNCs. Fortunately, most CNCs aggregations exhibit a regular spherical microstructure, even though broken spherical particles were observed. When the lowest CNCs concentration and inlet temperature (0.02 wt% and 140°C) were adopted, most of cellulose microspheres were broken, while regular cellulose microspheres can be observed in the SEM images (Fig. 5a). Within the investigated range, the increase of inlet temperature and CNCs concentration is favorable for the formation of cellulose microspheres, which can be confirmed by the increased ratio of regular cellulose microspheres. The cellulose microspheres tend to be broken when a lower inlet temperature and a lower CNCs concentration were adopted. On the other hand, with the increase of inlet temperature and low CNCs concentration, complete and regular cellulose microspheres were obtained. In addition, the broken cellulose spheres exhibited a hollow structure (Fig. 5a and Fig. 5d). The sheet-like CNCs can be observed in SEM images of some specimens, which may be according to the formation process of droplets as previously mentioned or the incomplete hydrolysis of sulfuric acid on cellulose.

Particle size and size distribution of cellulose microspheres

The particle size and size distribution of cellulose microspheres are important for future applications. Hence, the effect of CNCs concentration and inlet temperature on particle size and size distribution of cellulose microspheres were investigated, as shown in **Table I** and **Fig. 6**. The specific particle sizes (D10, D50, and D90) of cellulose microspheres are listed in Table I, and among them, D50 can be considered as the average particle size of specimens.

As shown in Fig. 6, the size distribution of specimens usually can be fitted into two or three peaks; the special qualities of spray drying may be responsible for it. As shown in Table I, cellulose microspheres with an average particle size of ca. 3 μm were obtained successfully. With the increase of CNCs concentration and inlet temperature, the average particle size of obtained cellulose microspheres was decreased. When the lowest CNCs concentration and

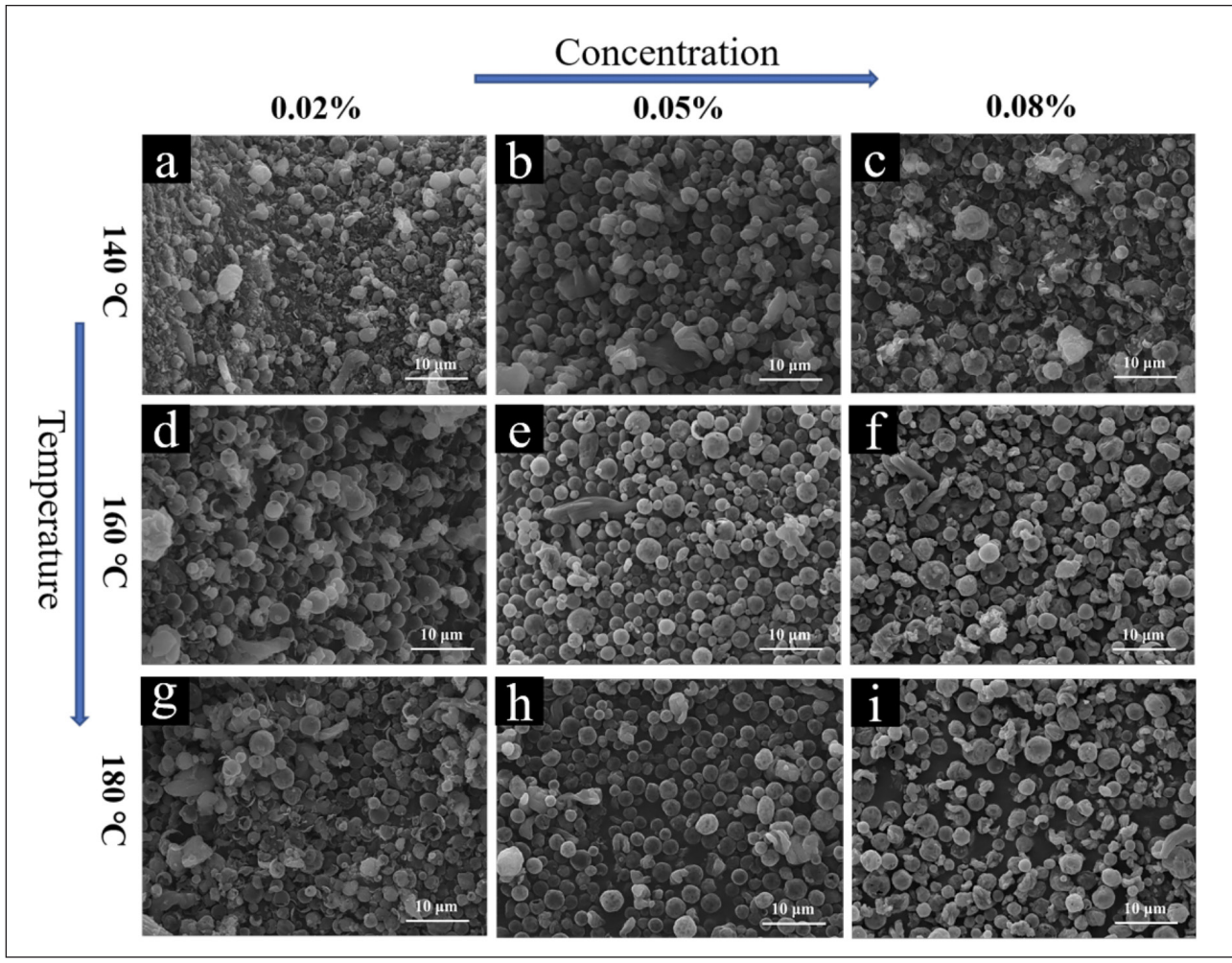

5. The SEM images of cellulose microspheres prepared by spray drying under different CNCs suspension concentrations and inlet temperatures.

inlet temperature were adopted, the average particle size of obtained cellulose microspheres was 50.72 ± 0.05 μm. At the same inlet temperature, the average particle size decreased to 6.99 ± 0.04 μm and 3.28 ± 0.09 μm when the adopted CNCs concentration was 0.05% and 0.08%, respectively. For the increased inlet temperature, the average particle size decreased from 3.28 ± 0.09 μm to 3.21 ± 0.01 μm and 3.18 ± 0.04 μm when the inlet temperature was increased from 140°C to 160°C and 180°C, respectively. In general, the effect of CNCs concentration on the average particle size of cellulose microspheres is more significant than that of inlet temperature on the same index.

Chemical structure and crystalline structure analysis

The chemical structure and crystalline structure of softwood fibers and cellulose microspheres were characterized by FTIR, as shown in **Fig. 7a** and Fig. 7b, and by XRD, as shown in **Fig. 8** and **Fig. 9**. The typical absorption peaks owing to cellulose are all present in the FTIR spectra of softwood fibers and cellulose microspheres. Among them, the absorption peaks near 3342 cm^{-1} and 2902 cm^{-1} are attributed to the O-H stretching vibration and C-H stretching vibration, respectively [28]. The C-O-C stretching of the pyran ring, the basic unit of cellulose, is responsible for the absorption peak at 1050 cm^{-1}. The absorption peaks at 1428 cm^{-1} and 1315 cm^{-1} correspond to the deformation and wagging vibration of -CH_2. The absorption peak at 894 cm^{-1} is owing to the bending vibration of C_1-H in the cellulose glycoside unit, which can be considered as the characteristic FTIR absorption peak of cellulose [29] The absorption peak at 1642 cm^{-1} is associated with the O-H bending of absorbed water [30]. During the sulfuric acid hydrolysis process, esterification between cellulose and sulfuric acid occurred, and the hydroxyl groups of cellulose were replaced by sulfhydryl groups. The esterification usually occurs on the C6 position of cellulose due to the higher activity of C6-OH [31]. Following sulfuric acid hydrolysis, two new absorption peaks at 1205 cm^{-1} and 815 cm^{-1} were present, which is attributed to the stretching vibration of the sulfate S=O group, as well as symmetrical C-O-S vibration of the C-O-SO_3 groups, indicating the partial replacement of hydroxyl

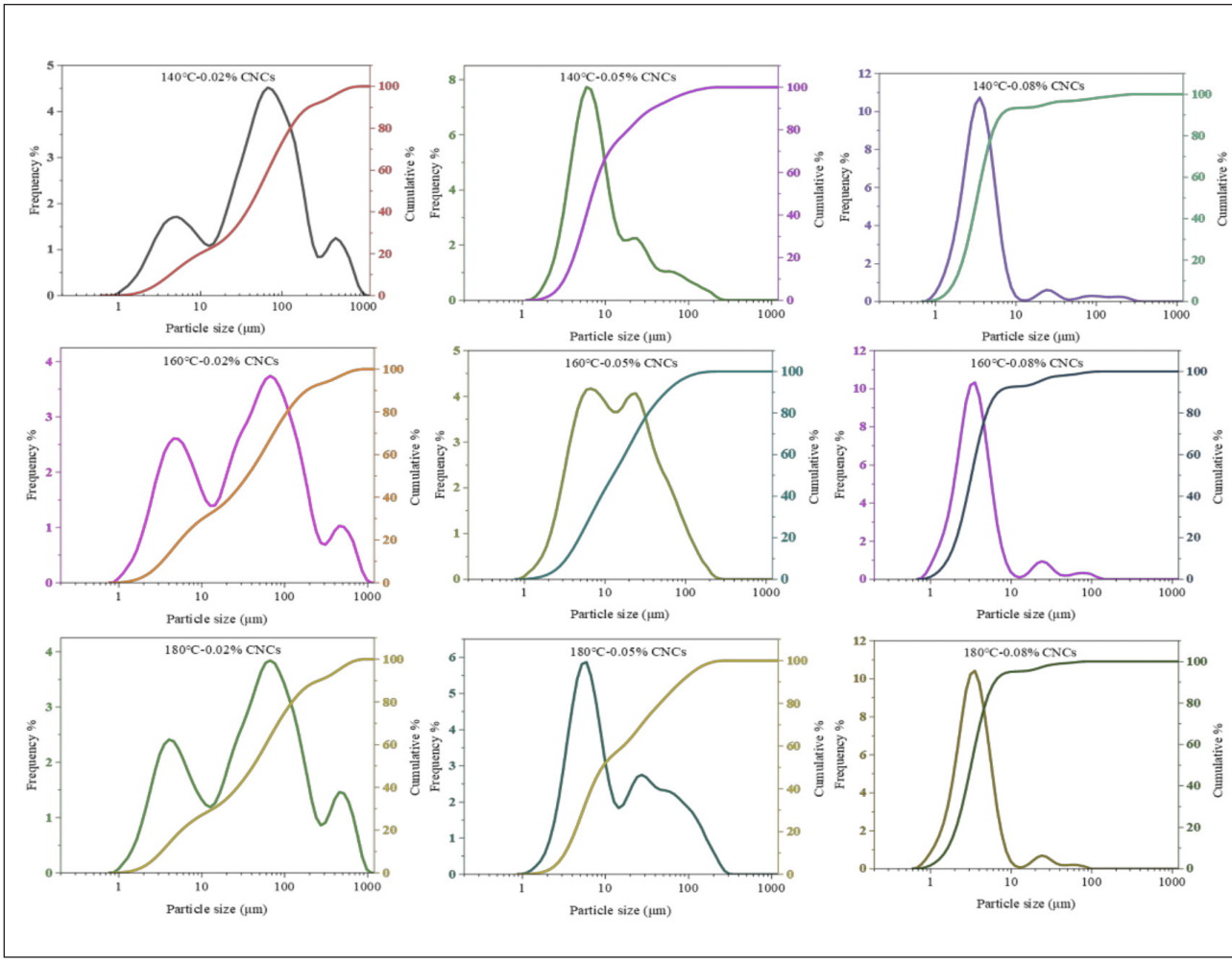

6. Size distribution of cellulose microspheres.

Sample	D10, μm	D50, μm	D90, μm
140°C–0.02% CNCs	4.23 ± 0.03	50.72 ± 0.05	211.20 ± 0.21
140°C–0.05% CNCs	3.22 ± 0.01	6.99 ± 0.04	36.93 ± 0.19
140°C–0.08% CNCs	1.75 ± 0.03	3.28 ± 0.09	6.56 ± 0.17
160°C–0.02% CNCs	3.33 ± 0.05	35.47 ± 0.05	182.90 ± 0.13
160°C–0.05% CNCs	3.34 ± 0.06	12.58 ± 0.02	56.87 ± 0.16
160°C–0.08% CNCs	1.66 ± 0.04	3.21 ± 0.01	6.92 ± 0.11
180°C–0.02% CNCs	3.28 ± 0.03	41.59 ± 0.08	255.60 ± 0.13
180°C–0.05% CNCs	3.27 ± 0.05	9.15 ± 0.06	80.90 ± 0.14
180°C–0.08% CNCs	1.63 ± 0.01	3.18 ± 0.04	6.24 ± 0.10

I. The specific particle sizes (D10, D50, and D90) of cellulose microspheres.

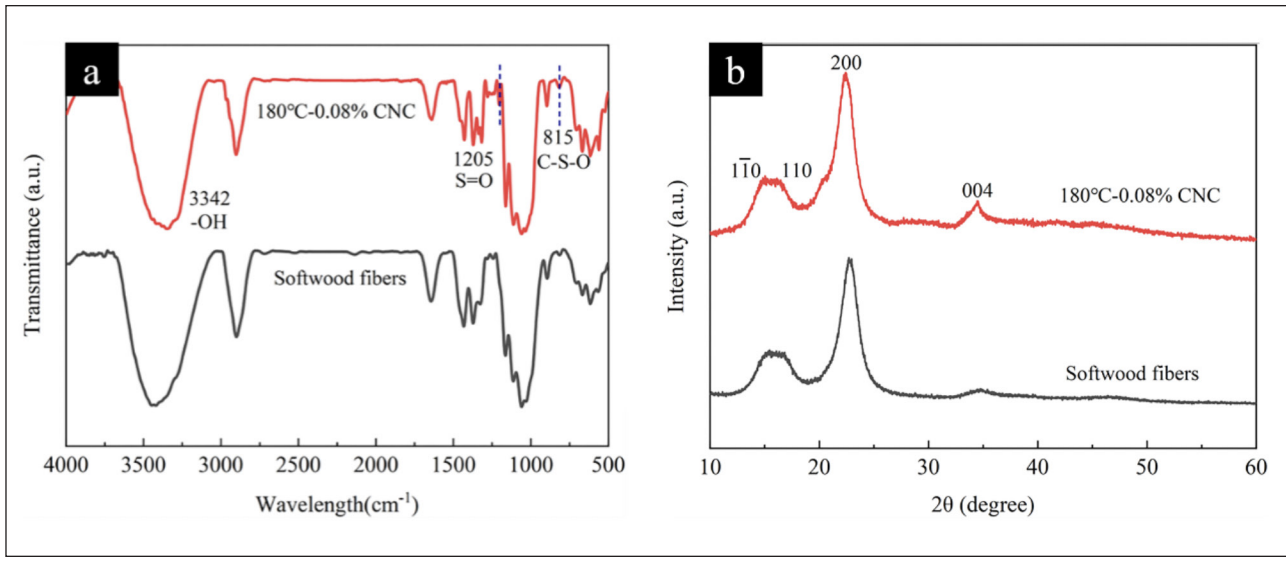

7. (a) Fourier transform infrared (FTIR) spectra and (b) X-ray diffractometer (XRD) patterns of cellulose microspheres and softwood fibers.

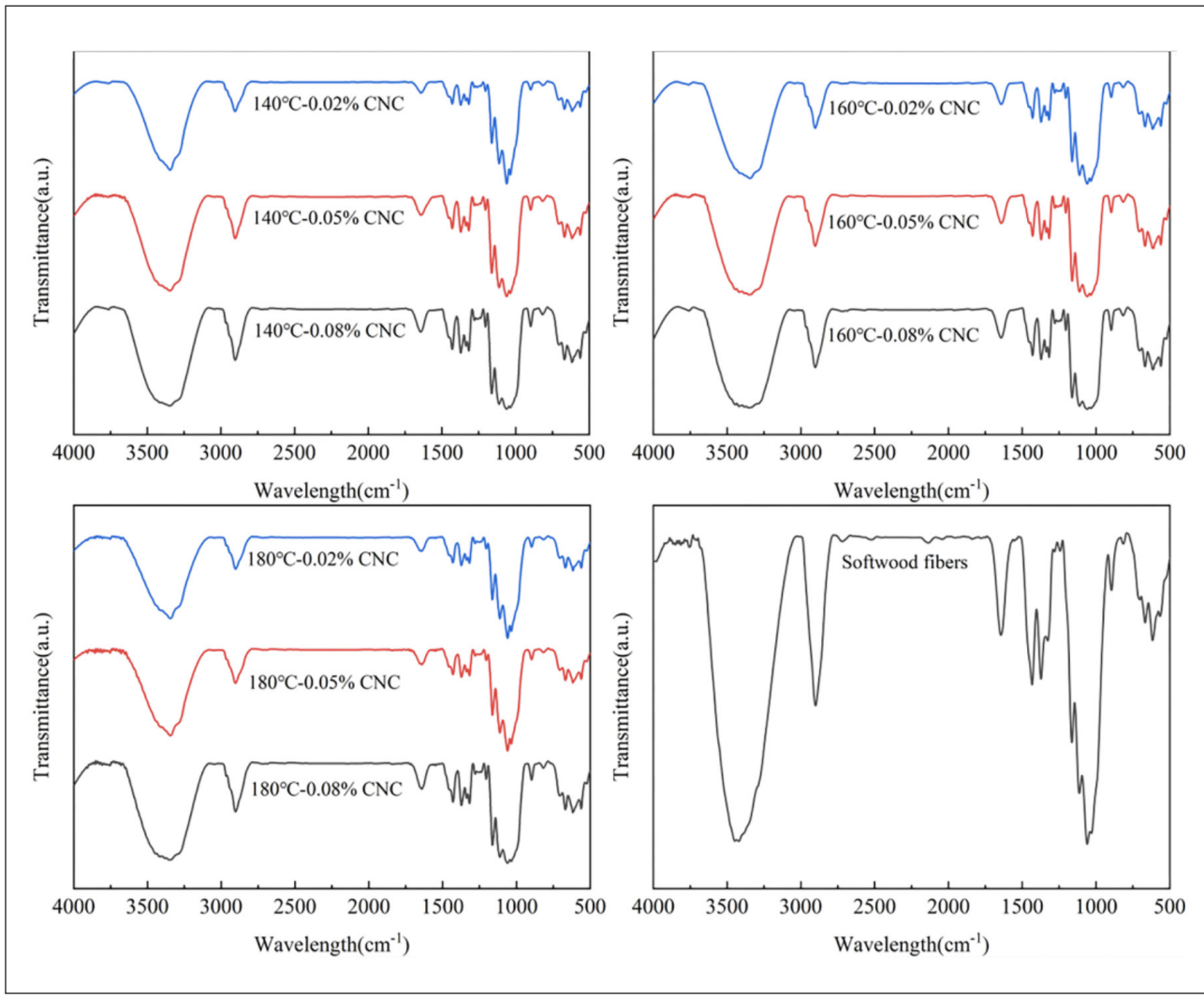

8. The FTIR analysis of cellulose microspheres and softwood fibers.

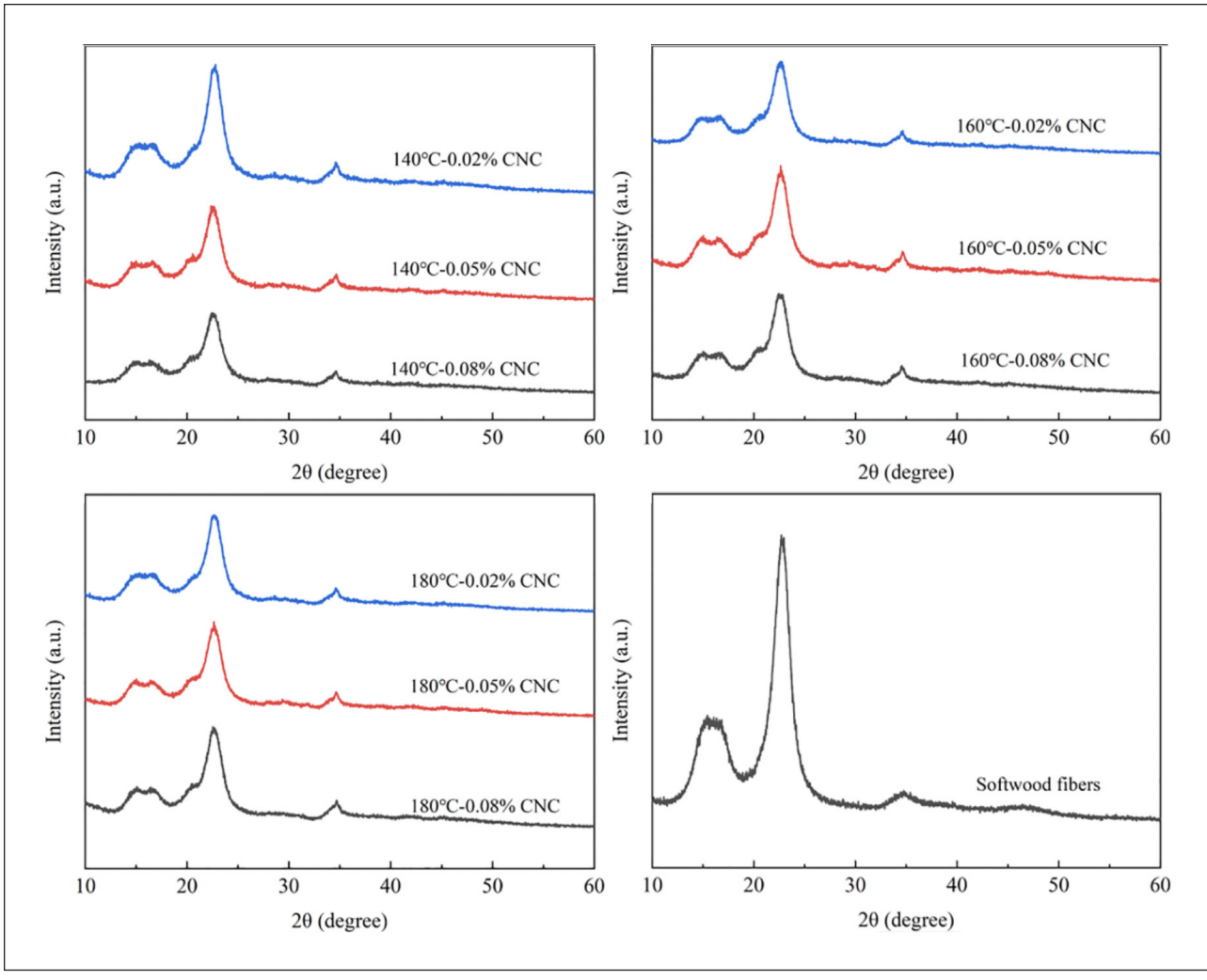

9. The XRD analysis of cellulose microspheres and softwood fibers.

groups by sulfhydryl groups. The introduced sulfhydryl groups provide a negative charge to CNCs, which is beneficial for the stable dispersion of CNCs suspension due to the repulsion of electrostatic force.

For the crystalline structure, all diffraction peaks attributed to cellulose I_β can be observed in the XRD pattern of softwood fibers and cellulose microspheres. Among them, the diffraction peaks were observed at near 2θ angles of approximately 14.8°, 16.5°, 22.6°, and 34.4°, corresponding to the (1 -1 0), (1 1 0), (2 0 0), and (0 0 4) crystal plane of the cellulose I_β [32], respectively, indicating the scarce variation in crystalline structure during the preparation and spray drying of CNCs. The most notable variation in the XRD pattern is the increased diffracted intensity of the (0 0 4) planes, which may be caused by the decreased particle size. However, due to the sulfuric acid hydrolysis, there was a discrepancy with the crystalline index (CI) of softwood fibers and cellulose microspheres. The higher CI of cellulose microspheres is rooted in the sulfuric acid hydrolysis process. During sulfuric acid hydrolysis, the accessible regions, i.e., amorphous regions and the surface of crystal regions of cellulose, will be hydrolyzed by acid [33,34]. Hence, the crystal regions are better prevented in the obtained CNCs, resulting in an increased CI of CNCs (**Table II**). The CI of cellulose microspheres with different spray-dried processes also exhibit discrepancy. With the increase of inlet temperature or the decrease of CNCs concentration, the CI of cellulose microspheres increase. The increased inlet temperature will lead to the more rapid evolution of water, as well as the more rapid formation of hydrogen bonding. The rapid formation of hydrogen bonding in a large amount leads to the increased CI of obtained cellulose microspheres.

Thermal stability analysis

The thermal stability of cellulosic materials is important for future applications. Hence, thermogravimetric (TG) analysis of cellulose microspheres and softwood fibers was carried out, as shown in **Fig. 10**. The start decomposition temperature, peak decomposition temperature, and residue

Sample	CI, %	Start Decomposition Temperature [a], °C	Peak Decomposition Temperature [b], °C	Residue Weight [c], %
Softwood fibers	63.08	280	356	11.91
140°C – 0.02% CNCs	71.53	258	287	21.35
140°C – 0.05% CNCs	68.57	264	315	16.69
140°C – 0.08% CNCs	67.24	250	268	19.07
160°C – 0.02% CNCs	72.33	252	264	20.40
160°C – 0.05% CNCs	70.10	259	289	16.60
160°C – 0.08% CNCs	69.17	242	267	19.23
180°C – 0.02% CNCs	72.77	245	269	26.27
180°C – 0.05% CNCs	72.50	247	269	19.40
180°C – 0.08% CNCs	69.53	253	263	26.08

[a] Start temperature using thermogravimetric analysis (TGA) results.

[b] Peak temperature of differential thermogravimetric (DTG) analysis.

[c] Residual weight at 800°C.

II. The crystalline index (CI), residue weight, and start and peak decomposition temperature of cellulose microspheres and softwood fibers.

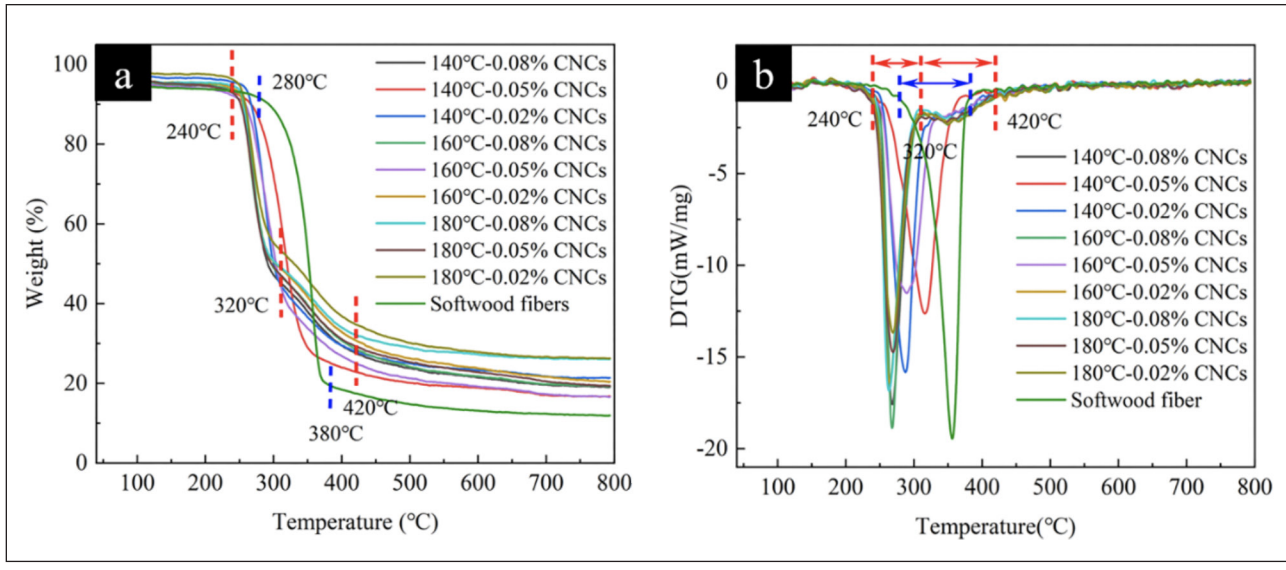

10. Thermal stability analysis of cellulose microspheres and softwood fiber: (a) thermogravimetric (TG) curves, and (b) differential thermogravimetric (DTG) curves.

weight at 800°C are listed in Table II. There are two main stages of weight loss of softwood fibers at the temperature range of 40°C–800°C. The approximate weight loss below 240°C is owing to the evaporation of water contained in the fibers. The decomposition of cellulose is responsible for the second stage of weight loss, which occurs at the temperature range of 240°C–380°C [29]. For cellulose microspheres, three main stages are present in the thermogravimetric/differential thermogravimetric (TG/DTG) curves. The water evaporation is also responsible for the weight loss of cellulose microspheres below 240°C. The decomposition of cellulose microspheres mainly occurs at the temperature range of 240°C–420°C, which involves the second and third stages of weight loss. These stages, at the temperature of 240°C–320°C and 320°C–420°C, can be clearly observed from the DTG curve, which is consistent with previous research [29,35]. The discrepancy between softwood fibers and cellulose microspheres at the temperature range of

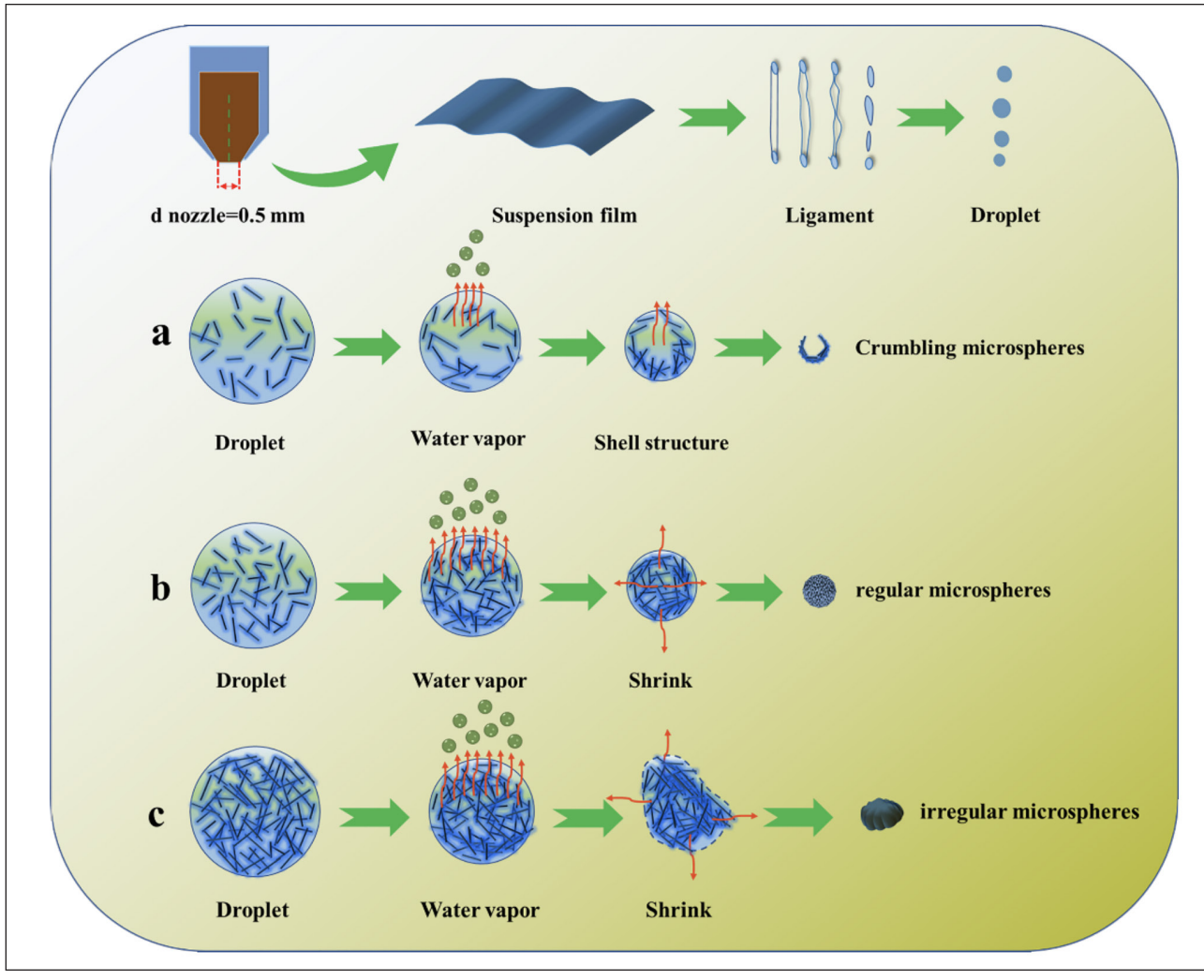

11. Formation mechanism of cellulose microspheres.

240°C–420°C is rooted in the sulfuric acid hydrolysis of cellulose. The carried sulfuric acid hydrolysis usually introduces sulfhydryl groups into cellulose chains, which are unfavorable for improvement in thermostability of cellulose, resulting in a decreased peak decomposition temperature (lower than 300°C) [30,36]. In addition, the unsulfated crystalline regions are responsible for the third weight loss (ca. 320°C) [30,36].

The start and peak decomposition temperatures of cellulose microspheres, as listed in Table II, were significantly lower than those of softwood fibers. The introduced sulfhydryl groups can reduce the activation energy during thermal degradation and then degrade the thermostability of cellulose microspheres, resulting in decreased start and peak decomposition temperature [37-39]. Moreover, the particle size of cellulosic materials also affects thermostability, which usually decreases to a certain extent with the decrease in particle size [40,41].

As listed in Table II, the thermostability of cellulose microspheres is lower than that of softwood fibers, but the residue weight of cellulose microspheres (16.60%~26.27%) is higher than that of softwood fibers (11.91%). The relatively high residue weights are attributed to the fact that the sulfhydryl groups, which are introduced during sulfuric acid hydrolysis, can act as a fire retardant for cellulose combustion and promote the char-forming capacity of cellulose microspheres during combustion by facilitating dehydration reactions [39,42]. In addition, thermal degradation usually occurs on the surface of cellulose microspheres first, and then a dense protective char layer can be formed, which also hinders the degradation of the internal cellulose component [20].

Formation mechanism of spherical structure

The formation process of CNCs aggregations from CNCs suspension, obtained by sulfuric acid hydrolysis, via spray drying is shown in **Fig. 11**. First, the CNCs suspension is passed through a circular nozzle to form a suspended film. Then, the high-speed hot air continues to break the suspended membrane into ligaments, forming droplets with diameters of a few micrometers to tens of micrometers [17]. The surface and internal water evaporates when the drop-

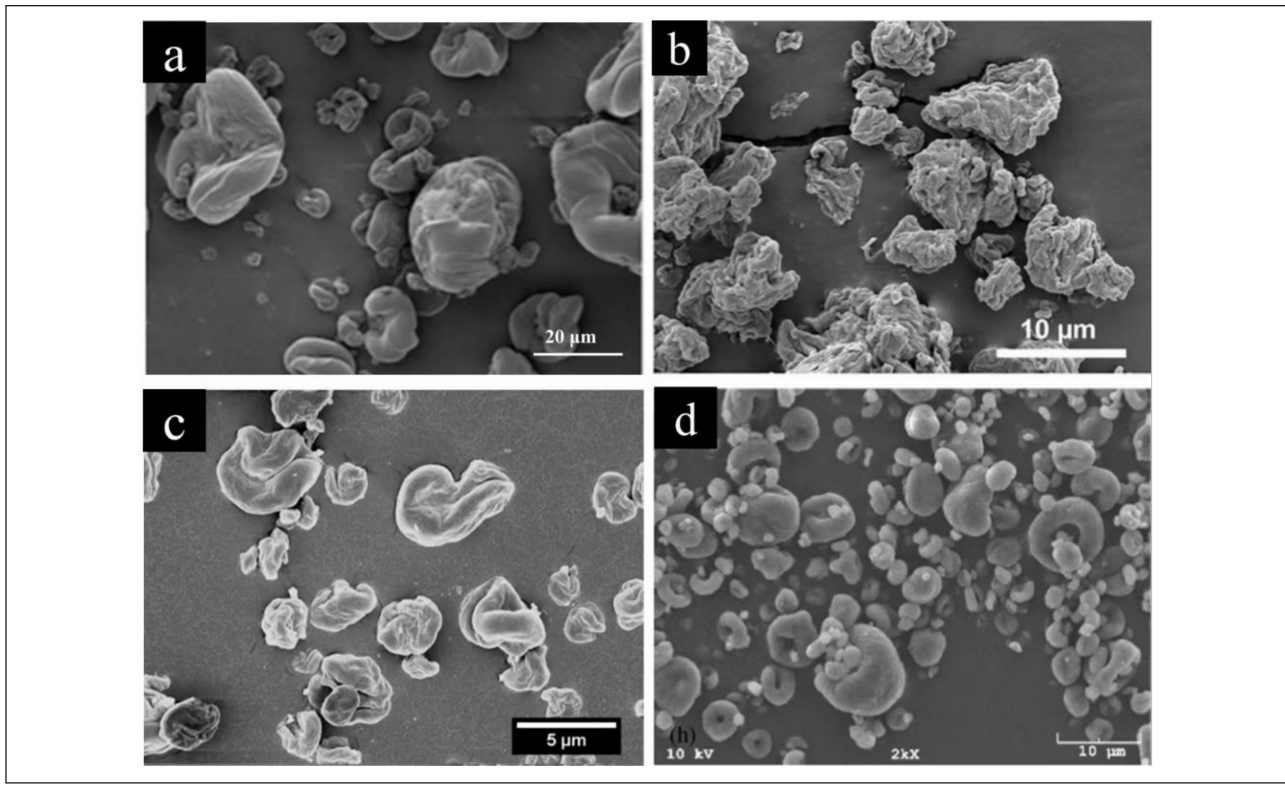

12. The SEM image of obtained cellulose microspheres in current literature by: (a) Abdallah and Kamal [26]; (b) Franca, de Barros, and Faez [23]; (c) Esparza et al. [43]; and (d) Peng, Han, and Gardner [21].

let passes through the drying chamber. Finally, the dried powder and moist air are separated by cyclone separation.

When the lower CNCs concentrations (0.05%) were adopted (Fig. 11a), most of the CNCs will be used to form the outer shell structure of the droplet, resulting in a lower content of CNCs inside. With the evaporation of water from the droplet surface, the CNCs concentration gradually increases, and accumulation or entanglement occurs. As a result, a shell (solid phase) structure is formed by the accumulated CNCs on the droplet surface, which further affects heat transfer and moisture evaporation [43-45]. Due to the relatively low CNCs content, a homogeneous and uniform outer shell structure cannot be formed, but a shell wall with varied thickness can be observed. Moreover, the shell structure formed by CNCs limits the diffusion of water vapor from the inside of the droplet to the surface. Hence, the diffusion of water vapor and the thin shell structure lead to the formation of broken particles.

When the higher CNCs suspension concentrations (0.08%) were adopted (Fig. 11b), CNCs were relatively more uniformly distributed on the surface and inside the droplet. The droplet tends to form regular spherical particles during the drying process. Unfortunately, with the further increase of CNCs concentration, CNCs cannot be converted into cellulose microspheres (Fig. 11c), and irregular particles were obtained. The amount of CNCs that can be contained in an individual droplet is limited. With the continual evaporation of water, the shrinkage of droplets occurs, and CNCs cannot be thoroughly contained in the individual droplet so irregular particles are obtained. In addition, the formation of hydrogen bonding can also accelerate the formation of irregular particles.

The effect of temperature on the formation of cellulose microspheres is mainly reflected in the influence on the rate of water evaporation. At a lower inlet temperature (140°C), the evaporation rate of water is relatively slow. With the increase of inlet temperature, the droplet undergoes wrinkling due to the accelerated evaporation rate, resulting in the reduction of particle size. Additionally, the morphological characteristics of CNCs also affect the formation of cellulose microspheres.

This study attempted to transform CNCs into cellulose microspheres by spray drying instead of an organic solvent process. Indeed, the spray-dried CNCs exhibited varied shapes. As reported by Abdallah et al. [26], CNCs with an average size of 171 ± 79.7 nm were transformed into nonporous, dense, and irregular particles via spray drying, which indicated that the controlled spray drying conditions may be essential for transforming CNCs to cellulose microspheres. Similarly, Esparza et al. [43] obtained irregular cellulosic particles (Fig. 12c) via spray drying with a CNC concentration of 1.7% and an inlet temperature of 220°C. Franca et al. [23] attempted to transform CNFs to cellulose microspheres encapsulating nitrogen and potassium nutrients. However, due to the lack of condition control during spray drying, the obtained cellulose particles exhibited ir-

regular shapes with a wrinkled surface. Peng et al. [21] systematically evaluated the effect of spray drying conditions, including gas flow rate, liquid feed rate, and suspension solid concentration, on the morphology of spray-dried CNCs particles. They obtained spray-dried CNCs in the shape of a mushroom cap (or doughnut) (Fig. 5d) when a gas flow rate of 540 L/h, feed rate of 8 mL/min, suspension concentration of 2%, and inlet temperature of 175°C were adopted. It is evident that the controlled spray drying conditions are beneficial for customizing the shape and size of obtained cellulose particles.

CONCLUSIONS

Cellulose microspheres with an average particle size of ca. 3 µm were successfully prepared using the spray drying method when the CNC size, concentration, and spray drying temperature were set at 106 nm, 0.08%, and 180°C, respectively. Particle size and concentration of CNCs and inlet temperature of spray drying have obvious effects on the microstructure of obtained cellulose microspheres. With the decrease of CNCs particle size, which took place via the increased hydrolysis time, the microstructure of obtained cellulosic particles become more and more regular. When the particle size of used CNCs is lower than 106 nm, cellulose microspheres are ultimately obtained via spray drying of CNCs. For the CNCs concentration, 0.1 wt% is the critical concentration for converting CNCs to cellulose microspheres. When the adopted concentration is larger than 0.1 wt%, cellulose microspheres cannot be formed, and only irregular particles are obtained. The average particle size of obtained cellulose spheres is affected by the inlet temperature and CNCs concentration, which is decreased with the increase of CNCs concentration and the increase of inlet temperature. The crystalline structure of cellulose microspheres is scarcely varied following sulfuric acid hydrolysis and spray drying. The introduction of sulfhydryl groups is confirmed by FTIR analysis. In addition, the introduced sulfhydryl groups are disadvantageous for the thermostability of obtained cellulose microspheres. On the whole, the conversion of CNCs to cellulose microspheres via a controlled spray drying process can be considered as a promising and controllable approach to obtain cellulose microspheres. **TJ**

ACKNOWLEDGEMENTS

This work was supported by the Shaanxi University of Science and Technology doctoral research startup fund project (BJ15-14); Shaanxi University of Science and Technology open subject of National Demonstration Center for Experimental Light Chemistry Engineering Education (2018QGSJ02-17); key research projects of Shaanxi Provincial Department of Education (19JZ016); and National Natural Science Foundation of China (201805178).

LITERATURE CITED

1. Tyagi, A. and Puravankara, S., *Mater. Adv.* 3(2): 810(2022). http://doi.org/10.1039/D1MA00731A.
2. Kumar, S., Srivastava, R., Pak, D., et al., *Int. J. Energy Res.* 45(10): 14389(2021). http://doi.org/10.1002/er.6771.
3. Wu, J. and Andrews, M.P., *J. Mater. Chem. A* 12(2): 950(2024). http://doi.org/10.1039/D3TA05298B.
4. Zhao, L., Li, S., Liang, C., et al., *Biochem. Eng. J.* 166:107826(2021). http://doi.org/10.1016/j.bej.2020.107826.
5. Fan, J.-B., Huang, C., Jiang, L., et al., *J. Mater. Chem.* B 1(17): 2222(2013). http://doi.org/10.1039/C3TB00021D.
6. Wang, S., Lu, A., and Zhang, L., *Prog. Polym. Sci.* 53: 169(2016). http://doi.org/10.1016/j.progpolymsci.2015.07.003.
7. Xie, H., Du, H., Yang, X., et al., *Int. J. Polym. Sci.* 2018(1): 7923068(2018). http://doi.org/10.1155/2018/7923068.
8. Thümmler, K., Fischer, S., Feldner, A., et al., *Cellulose* 18: 135(2011). http://doi.org/10.1007/s10570-010-9465-z.
9. Zhu, H.F., Zhu, E.W., Xie, Y.Y., et al., *Carbohydr. Polym.* 296: 8(2022). http://doi.org/10.1016/j.carbpol.2022.119947.
10. Pei, X.L., Li, Y., Lu, L.J., et al., *ACS Appl. Mater. Interfaces* 13(37): 44418(2021). http://doi.org/10.1021/acsami.1c12850.
11. Wu, S.M., Gong, Y.Q., Liu, S.L., et al., *Carbohydr. Polym.* 254: 8(2021). http://doi.org/10.1016/j.carbpol.2020.117421.
12. Xu, Y., Xu, Y., Chen, H., et al., *Carbohydr. Polym.* 294: 119830(2022). http://doi.org/10.1016/j.carbpol.2022.119830.
13. Snyder, H.E. and Lechuga-Ballesteros, D., "Spray drying: Theory and pharmaceutical applications," in *Pharmaceutical Dosage Forms: Tablets*, Vol. I, Unit Operations and Mechanical Properties (L.L. Augsburger and S.W. Hoag, Eds.), CRC Press, Boca Raton, FL, USA, 2008, Chap. 7. https://doi.org/10.3109/9781420020281.
14. Ziaee, A., Albadarin, A.B., Padrela, L., et al., *Eur. J. Pharm. Sci.* 127: 300(2019). http://doi.org/10.1016/j.ejps.2018.10.026.
15. Cal, K. and Sollohub, K., *J. Pharm. Sci.* 99(2): 575(2010). http://doi.org/10.1002/jps.21886.
16. Santos, D., Maurício, A.C., Sencadas, V., et al., "Spray drying: An overview," in *Biomaterials – Physics and Chemistry – New Edition* (R. Pignatello and T. Musumeci, Eds.), InTechOpen, Rijeka, 2018. http://doi.org/10.5772/intechopen.72247.
17. Yang, G., Ma, G., He, M., et al., *Nanomaterials* 11(2): 439(2021). http://doi.org/10.3390/nano11020439.
18. Peng, Y.C., Gardner, D.J., and Han, Y.S., *Cellulose* 19(1): 91(2012). http://doi.org/10.1007/s10570-011-9630-z.
19. Peng, Y., Gardner, D.J., Han, Y., et al., *J. Colloid Interface Sci.* 405: 85(2013). http://doi.org/10.1016/j.jcis.2013.05.033.
20. Peng, Y., Gardner, D.J., Han, Y., et al., *Cellulose* 20: 2379(2013). http://doi.org/10.1007/s10570-013-0019-z.
21. Peng, Y.C., Han, Y.S., and Gardner, D.J., *Wood Fiber Sci.* 44(4): 448(2012).
22. Peng, Y. and Gardner, D.J., *TAPPI J.* 14(9): 565(2015). http://doi.org/10.32964/TJ14.9.565.
23. França, D., de Barros, J.R.S., and Faez, R., *Cellulose* 28(3): 1571(2021). http://doi.org/10.1007/s10570-020-03609-5.
24. Zhu, Z., Fu, S., and Lucia, L.A., *ACS Sustainable Chem. Eng.* 7(5): 5376(2019). http://doi.org/10.1021/acssuschemeng.8b06399.

25. Segal, L., Creely, J.J., Martin, A.E., et al., *Text. Res. J.* 29(10): 786(1959). http://doi.org/10.1177/004051755902901003.
26. Abdallah, W. and Kamal, M.R., *Cellulose* 25(10): 5711(2018). http://doi.org/10.1007/s10570-018-1975-0.
27. Alarcón-Moyano, J., Acuña, D., Matiacevich, S., et al., *Food Hydrocolloids* 140: 10(2023). http://doi.org/10.1016/j.foodhyd.2023.108571.
28. Bastante, C.C., Silva, N.H.C.S., Cardoso, L.C., et al., *Food Hydrocolloids* 117: 106709(2021). http://doi.org/10.1016/j.foodhyd.2021.106709.
29. Zhang, H., Chen, Y., Wang, S., et al., *Carbohydr. Polym.* 238: 116180(2020). http://doi.org/10.1016/j.carbpol.2020.116180.
30. Dai, H., Ou, S., Huang, Y., et al., *Cellulose* 25: 1743(2018). http://doi.org/10.1007/s10570-018-1671-0.
31. Henschen, J., Li, D., and Ek, M., *Carbohydr. Polym.* 213: 208(2019). http://doi.org/10.1016/j.carbpol.2019.02.056.
32. Wang, J., Xu, J., Zhu, S., et al., *Carbohydr. Polym.* 251: 117094(2021). http://doi.org/10.1016/j.carbpol.2020.117094.
33. Kassab, Z., Abdellaoui, Y., Salim, M.H., et al., *Carbohydr. Polym.* 245: 116506(2020). http://doi.org/10.1016/j.carbpol.2020.116506.
34. Lim, W.-L., Gunny, A.A.N., Kasim, F.H., et al., *Cellulose* 28(10): 6183(2021). http://doi.org/10.1007/s10570-021-03914-7.
35. Goh, K.Y., Ching, Y.C., Chuah, C.H., et al., *Cellulose* 23: 379(2016). http://doi.org/10.1007/s10570-015-0812-y.
36. Teixeira de Morais, E., Bondancia, T.J., Teodoro, K.B.R., et al., *Ind. Crops Prod.* 33(1): 63(2011). http://doi.org/10.1016/j.indcrop.2010.08.009.
37. D'Acierno, F., Hamad, W.Y., Michal, C.A., et al., *Biomacromolecules* 21(8): 3374(2020). http://doi.org/10.1021/acs.biomac.0c00805.
38. Roman, M. and Winter, W.T., *Biomacromolecules* 5(5): 1671(2004). http://doi.org/10.1021/bm034519.

ABOUT THIS PAPER

Cite this article as:
Meng, Q., Zheng, W., and Xu, Y., *TAPPI J.* 24(2): 74(2025). https://doi.org/10.32964/TJ24.2.74

DOI: https://doi.org/10.32964/TJ24.2.74

ISSN: 0734-1415

Publisher: TAPPI Press

39. Zhao, G., Du, J., Chen, W., et al., *Cellulose* 26: 8625(2019). http://doi.org/10.1007/s10570-019-02683-8.
40. Liu, W., Du, H., Liu, H., et al., *ACS Sustainable Chem. Eng.* 8(44): 16691(2020). http://doi.org/10.1021/acssuschemeng.0c06561.
41. Wang, H., Du, H., Liu, K., et al., *Carbohydr. Polym.* 266: 118107(2021). http://doi.org/10.1016/j.carbpol.2021.118107.
42. Johar, N., Ahmad, I., and Dufresne, A., *Ind. Crops Prod.* 37(1): 93(2012). http://doi.org/10.1016/j.indcrop.2011.12.016.
43. Esparza, Y., Ngo, T.D., Fraschini, C., et al., *Ind. Eng. Chem. Res.* 58(43): 19926(2019). http://doi.org/10.1021/acs.iecr.9b03951.
44. Handscomb, C.S., Kraft, M., and Bayly, A.E., *Chem. Eng. Sci.* 64(4): 628(2009). http://doi.org/10.1016/j.ces.2008.04.051.
45. Lintingre, E., Lequeux, F., Talini, L., et al., *Soft Matter* 12(36): 7435(2016). http://doi.org/10.1039/c6sm01314g.

ABOUT THE AUTHORS

The microstructure of cellulose plays a crucial role in material applications. Therefore, it is of great significance to explore the morphology and structural changes of cellulose. The controlled conversion of cellulose nanocrystals (CNCs) into cellulose microspheres by spray drying technology is a promising method. In this paper, the conditions for the controlled conversion of CNCs into cellulose microspheres were systematically studied, and the effects of key indicators such as CNCs particle size, drying concentration, and spray drying temperature on the morphology and structure of cellulose microspheres were studied.

The most difficult part of this research was control of the morphology and structure of cellulose microspheres. We solved this problem by finding data and experimental exploration.

We found that the size and concentration of CNCs have significant effects on the morphology and structure of cellulose microspheres. The most surprising finding was the transformation of rod-like CNCs into spherical cellulose, which increases the application potential of cellulose.

Cellulose microspheres may have good application potential in food, medicine, adsorption, and other fields. Our next step will be to further explore the preparation and application of functional cellulose microspheres.

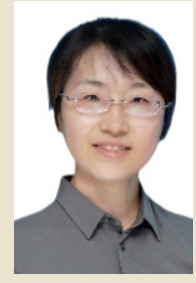

Meng

Zheng

Xu

Meng is senior engineer and Zheng is a graduate student in the College of Bioresource Chemical and Materials Engineering at Shaanxi University of Science and Technology in Xi'an, China. Xu is a lecturer in the College of Bioengineering at Sichuan University of Science and Engineering in Yibin, China. Email Meng at mengqingjun@sust.edu.cn and Xu at ppxuyang@126.com.